# Effect of Austempering Time on Mechanical Properties of a Low Manganese Austempered Ductile Iron

*Susil K. Putatunda and Pavan K. Gadicherla*

(*Submitted 7 June 1999; in revised form 18 October 1999*)

**An investigation was carried out to examine the influence of austempering time on the resultant microstructure and the room-temperature mechanical properties of an unalloyed and low manganese ductile cast iron with initially ferritic as-cast structure. The effect of austempering time on the plane strain fracture toughness of this material was also studied. Compact tension and round cylindrical tensile specimens were prepared from unalloyed ductile cast iron with low manganese content and with a ferritic as-cast (solidified) structure. These specimens were then austempered in the upper (371 °C) and lower (260 °C) bainitic temperature ranges for different time periods, ranging from 30 min. to 4 h. Microstructural features such as type of bainite and the volume fraction of ferrite and austenite and its carbon content were evaluated by X-ray diffraction to examine the influence of microstructure on the mechanical properties and fracture toughness of this material.**

**The results of the present investigation indicate that for this low manganese austempered ductile iron (ADI), upper ausferritic microstructures exhibit higher fracture toughness than lower ausferritic microstructures. Yield and tensile strength of the material was found to increase with an increase in austempering time in a lower bainitic temperature range, whereas in the upper bainitic temperature range, time has no significant effect on the mechanical properties. A retained austenite content between 30 to 35% was found to provide optimum fracture toughness. Fracture toughness was found to increase with the parameter $(X\gamma C\gamma/d)^{1/2}$, where $X\gamma$ is the volume fraction of austenite, $C\gamma$ is the carbon content of the austenite, and $d$ is the mean free path of dislocation motion in ferrite.**

**Keywords** austempering, ductile iron

## 1. Introduction

Austempered ductile iron (ADI) has attracted considerable interest in recent years because of its excellent mechanical properties such as high strength with good ductility,[1–3] good wear resistance,[4,5] and good fatigue properties.[6–9] It is therefore considered as an economical substitute for wrought or forged steel in several structural applications, especially in the automotive industry.[10–12] The remarkable properties of ADI are attributed to its unique microstructure consisting of high carbon austenite ($\gamma_{HC}$) and ferrite ($\alpha$). Ductile or nodular cast iron when subjected to austempering heat treatment produces a microstructure consisting of ferrite ($\alpha$) and high carbon austenite ($\gamma_{HC}$). This is different from steel. When steel is austempered, the resulting microstructure consists of fine dispersion of carbide in a ferritic matrix called bainite. In ductile cast iron, the presence of a large amount of silicon suppresses the carbide formation. Because of this difference, austempered structure in ductile cast iron is often referred to as "ausferritic" rather than bainitic. When ferrite forms within the austenite during the austempering process of nodular or ductile cast iron, the carbon is rejected from these regions and goes into solution in the surrounding austenite. As more and more ferrite forms, the carbon content of the austenite increases. Since the carbon content of this austenite is very high (in excess of 1.0%), the austenite is stable in room temperature and hence the resulting microstructure consists of ferrite and high carbon and stable austenite. This is the desired microstructure in ADI. However, if the austempering reaction is carried out for too long, a stage II or second reaction sets in during which the high carbon austenite ($\gamma_{HC}$) can further decompose into ferrite and carbide. This reaction is undesirable because of the embrittling effect[2] of carbides. Therefore, best mechanical properties are obtained in ADI after completion of the first reaction but before the onset of the second reaction. This time interval between the completion of the first reaction and the onset of the second reaction is known as the process window. The process window can be enlarged by the addition of alloying elements such as nickel and molybdenum. Therefore, conventional ADI has some nickel (1.5%) and molybdenum (0.3%) present in it. The microstructure of ADI depends on the austempering temperature and time. The important microstructural features are the morphology of ferrite, retained austenite content, carbon content of austenite, and presence or absence of carbides in austenite or ferrite.

Successful application of ADI as a structural component requires optimization of its mechanical properties, especially fracture toughness. Fracture toughness is a measure of a material's resistance[13] to crack growth under sustained monotonic loading condition. Fracture toughness is therefore an extremely important parameter for structural design, since structural components designed on the basis of fracture toughness are not expected to undergo catastrophic failure in service. Several investigators[14–22] in the past have studied the influence of heat treatment parameters on the fracture toughness of ADI. However, most of these studies have been carried out on ADI of conventional composition, *i.e.*, ductile cast iron containing alloying elements such as nickel and molybdenum and relatively high manganese content

**Susil K. Putatunda,** Department of Chemical Engineering and Materials Science, Wayne State University, Detroit, MI 48202; and **Pavan K. Gadicherla,** Department of Chemical Engineering and Materials Science, Wayne State University, Detroit, MI 48202.

(Mn = 0.4%). Recent studies by some investigators[23,24] have shown that alloying elements such as manganese and molybdenum promote segregation in ADI. These segregated regions draw large amounts of carbon, and during austempering, these regions may transform into martensite and lead to poor mechanical properties. Therefore, ductile cast iron and without any alloying elements and low manganese content may provide better mechanical properties as a result of austempering heat treatment process. However, very little information is available in the literature on the effect of austempering on the microstructure and mechanical properties of such alloys (unalloyed ductile cast iron and with low manganese content). The present investigation was therefore undertaken to examine the influence of austempering heat treatment on the microstructure and the mechanical properties of an unalloyed ductile cast iron with low manganese content. A predominantly ferritic as-cast (solidified) structure was chosen for this investigation because most of the studies[14–22] so far on ADI have been carried out on ductile cast iron with pearlitic as-cast structure. However, cooling rate and alloying elements can significantly affect the as-cast microstructure. It is of great interest to examine the heat treatment response of nodular cast iron with ferritic as-cast microstructure. In two previous publications by these authors,[25,26] the influence of austempering temperature[25] and austenitizing temperature[26] on the mechanical properties of this unalloyed low manganese ADI with ferrite as-cast structure has been discussed. The present paper is a continuation of the above study, where the influence of austempering time in the upper and lower bainitic regions on the microstructure and mechanical properties (including fracture toughness) of the above alloy has been examined.

## 2. Experimental Procedure

### 2.1 Material

The chemical composition of the nodular cast iron used in the present investigation is reported in Table 1. The material was sand cast in the form of slabs (370 × 100 × 140 mm). The microstructure of the as-cast material is shown in Fig. 1. The as-cast microstructure was predominantly ferritic (in excess of 80%) in nature. The presence of graphite nodules can also be seen in this microstructure.

Round cylindrical tensile samples were prepared from cast slabs per ASTM standard E-8.[27] In addition, compact tension specimens for fracture toughness tests were fabricated per ASTM standard E-399.[13] The details of the compact tension as well as tensile specimens have been reported elsewhere.[20–22] After fabrication, these specimens were initially austenitized at 927 °C for 2 h and then subsequently austempered at 260 and 371 °C for 30 min, 60 min, 2 h, 3 h, and 4 h, respectively. The austempering temperatures were so selected because 260 °C was expected to produce a lower bainitic (lower ausferritic) microstructure, while 371 °C was expected to result in an upper bainitic (upper ausferritic) microstructure. Different austempering time was selected to obtain a variation in carbon content of retained austenite at each of these temperatures.

**Table 1 Chemical composition of the material (wt.%)**

| | |
|---|---|
| C | 3.44 |
| Si | 2.41 |
| Mn | 0.15 |
| S | 0.007 |
| P | 0.015 |
| Mg | 0.164 |

### 2.2 X-ray

The microstructures of the heat treated samples were studied by optical microscopy after etching with 2% nital solution. The volume fraction of retained austenite and its carbon content in all these samples were determined by X-ray diffraction following the procedure of Rundman and Klug.[28] X-ray diffraction profiles were obtained on a Rigaku rotating head anode diffractometer at 40 kV and 100 mA using copper K radiation. The samples were scanned in the angular $2\Theta$ range of 42 to 46 deg and 70 to 105 deg. The profiles were analyzed in a computer to obtain peak positions as well as the integrated intensities. Volume fraction of the austenite was determined by direct comparison methods[29] using integrated intensities of (210) and (211) peaks of ferrite and (111), (220), and (311) peaks of austenite. The carbon content of the austenite was determined using the following relationship:[30]

$$a_\gamma = 0.3548 + 0.0044C_\gamma \quad \text{(Eq 1)}$$

where $a_\gamma$ is the lattice parameter of austenite in nanometers and $C_\gamma$ is its carbon content in weight percent. (111), (220), and (311) peaks of austenite were used in estimating the lattice parameter of austenite.

### 2.3 Mechanical Testing

Fracture toughness testing was carded out per ASTM standard E-399[13] using a servohydraulic MTS-810 (MTS System, Minneapolis, MN) test machine. The specimens were precracked in fatigue at a $\Delta K$ level of 15 MPa $\sqrt{m}$ to produce a 2 mm long sharp reproductable crack front. The specimens were then loaded in tension and the load displacement diagrams were obtained using a

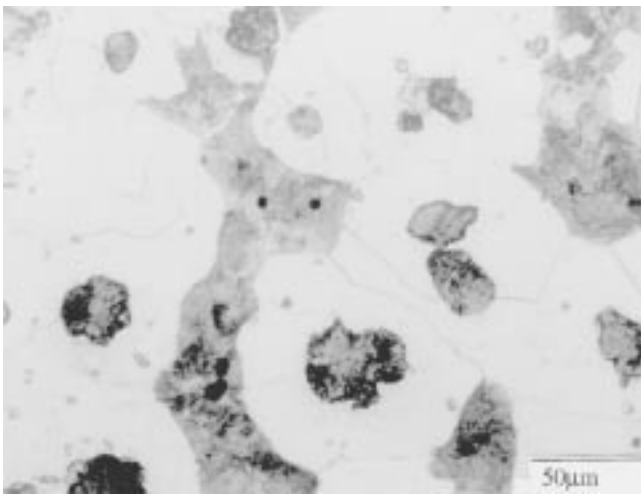


**Fig. 1** Microstructure of the material in as-cast condition. Magnification 1000X

clip gage at the crack mouth of the specimens. The $P_Q$ values were calculated using the 5% secant deviation technique, and these were used for calculating the $K_Q$ values using, the standard intensity factor calibration function for compact tension specimens.[13] Five identical samples were tested from each heat-treated condition. Values reported here are average values from these five tests. Since the $K_Q$ values satisfied all the conditions of a valid $K_{IC}$ test, these are all valid $K_{IC}$ values.

Tensile tests were carried out per ASTM standard E-8[27] at a constant engineering strain rate of $4*10^{-4}$ $s^{-1}$ on an MTS 810 servohydraulic test machine. Five samples were tested in each case and load displacement diagrams were obtained on an *X-Y* plot. From these load displacement diagrams, yield strength, ultimate tensile strength, and percentage elongation were calculated. The average values from five test samples are reported here.

Fractographic examinations were carried out on the fracture surfaces of the fracture toughness samples on a Hitachi S-2400 (Tokyo, Japan) scanning electron microscope to identify the fracture mode.

## 3. Results and Discussions

### 3.1 Microstructure

Some of the representatives of the microstructures of the samples austempered at two different temperatures for different time periods are shown in Fig. 2 and 3. While Fig. 2(a) to (d) report microstructures of samples austempered at 260 °C, Fig. 3 (a) to (c) report the microstructures of the samples after austempering at 371 °C for different time periods. When comparing the microstructures at a fixed time period, it is evident that the samples austempered at lower temperature (260 °C) showed acicular ferrite characteristics of (lower bainitic) lower ausferritic

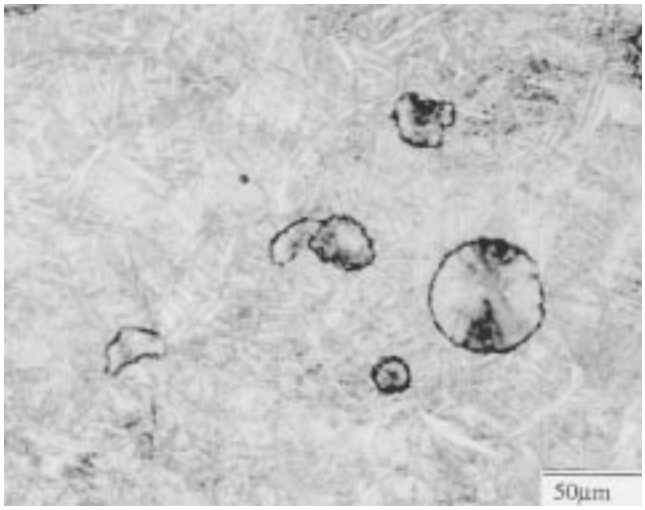


**(a)**

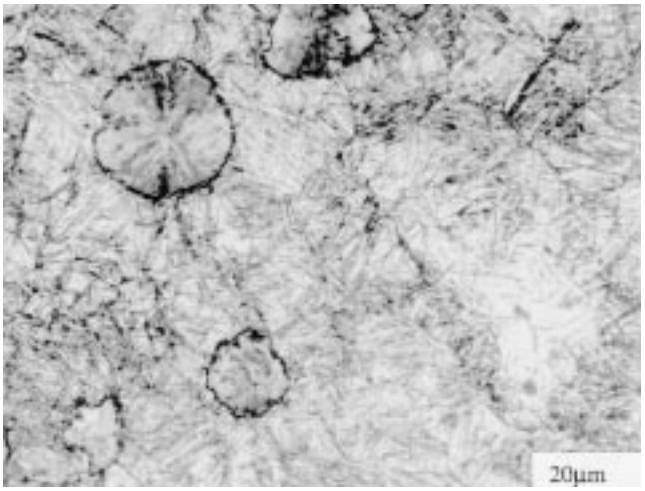


**(c)**

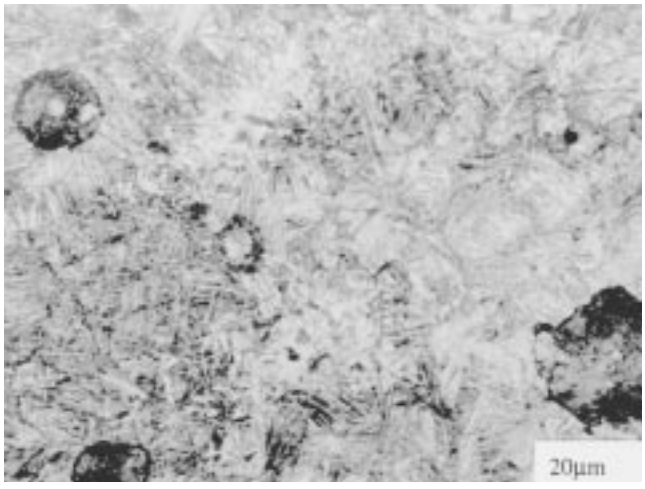


**(b)**

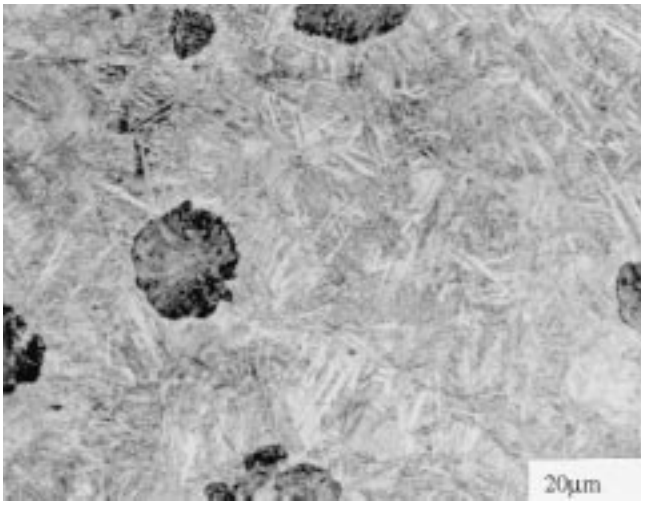


**(d)**

**Fig. 2** **(a)** Microstructure of the material austempered at 260 °C for 30 min. Magnification 400X. **(b)** Microstructure of the material austempered at 260 °C for 1 h. Magnification 400X. **(c)** Microstructure of the material austempered at 260 °C for 3 h. Magnification 400X. **(d)** Microstructure of the material austempered at 260 °C for 4 h. Magnification 400X

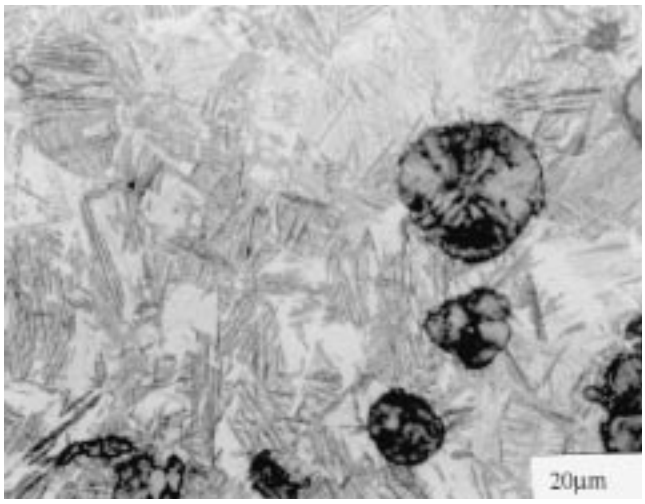


**(a)**

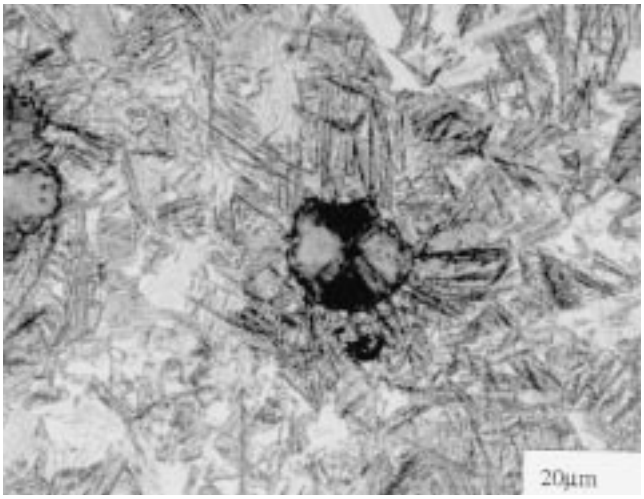


**(b)**

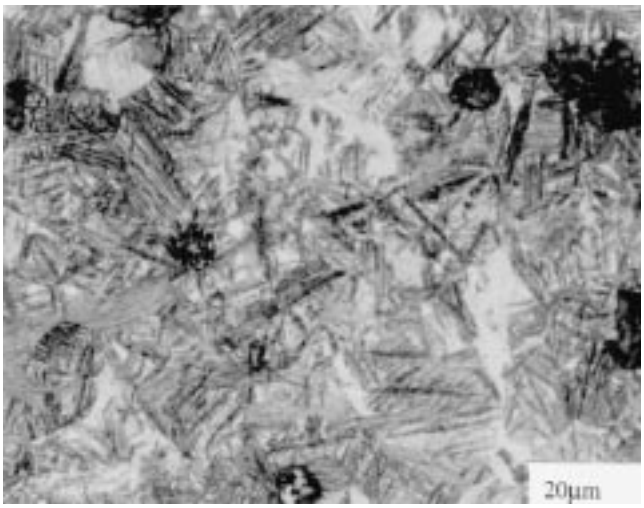


**(c)**

**Fig. 3** **(a)** Microstructure of the material austempered at 371 °C for 30 min. Magnification 400X. **(b)** Microstructure of the material austempered at 260 °C for 1 h. Magnification 400X. **(c)** Microstructure of the material austempered at 371 °C for 3 h. Magnification 400X

microstructure, while those austempered at 371 °C showed broad feathery-type ferrite characteristics of (upper bainitic) upper ausferritic microstructure. Or, in other words, as the austempering temperature has increased from 260 to 371 °C, both the ferrite and austenite has coarsened as a result of austempering process. Microstructures also reveal some coarsening of the ferrite and austenite as the austempering time increases. However, the rate of coarsening was greater at higher temperature (371 °C) than at lower temperature (260 °C). The volume fraction of austenite as well as its carbon content was determined by X-ray diffraction. These are reported in Fig. 4 and 5 for both upper and lower ausferrite microstructures. Figure 4 reveals that for the same time period of austempering, the austenite content was higher at higher austempering temperature (371 °C) than at 260 °C. While the austenite content was between 30 and 36% at 371 °C, it was only 12 to 18% at 260 °C. During the austempering process, ferrite forms out of austenite by nucleation and grain growth process.[2,18,20] Since at lower austempering temperature (260 °C) super cooling is larger, the nucleation rate is greater and, consequently, more ferrite is nucleated at lower temperature. As a result, the ferrite content, is greater or, in other words, the austenite content is lower at lower austempering temperature (260 °C). On the other hand, at higher austempering temperature (371 °C) super cooling is lower, and hence less ferrite is nucleated. Consequently, the microstructure contains a lower volume fraction of ferrite, *i.e.*, a larger volume fraction of austenite. Furthermore, as ferrite forms, carbon has to diffuse out for ferrite to grow. Since diffusion of carbon depends on temperature, at lower austempering temperature (260 °C), the diffusion of carbon from regions transforming into ferrite to the surrounding austenite is lower than that at higher temperature (371 °C). Consequently, ferrite needles are finer at lower temperature (260 °C), but both ferrite and austenite are coarser at the higher temperature (371 °C). This is clearly evident in the microstructures reported in Fig. 2 and 3.

An estimate of the mean particle size of ferrite, *d*, was determined from the breadth of the (211) diffractometer peak of the ferrite using the Scherrer formula:[29]

$$d = 0.9\lambda/\beta \cos\theta$$

where $d$ is the mean particle size, $\lambda$ is the wavelength, $\Theta$ is the Bragg angle, and $\beta$ is the peak breadth at half-height in radians. Figure 6 reports the $d$ values of all the samples after austempering for different time periods at two austempering temperatures. The mean particle size $d$ is a measure of mean free path of dislocation motion within this ferrite phase. Figure 6 shows that $d$ values are smaller at lower austempering temperature and are not significantly affected by austempering time. However, at higher austempering temperature (371 °C), $d$ values are much larger than at 260 °C and they increase significantly with an increase in time. This increase in $d$ values at 371 °C is indicative of rapid grain coarsening at this temperature.

Figure 4 also shows the variation in volume friction of austenite with time. The volume fraction of austenite was found to decrease at 260 °C with an increase in austempering time. This gradual decrease in austenite content is due to increased carbon diffusion with time. As the carbon diffuses out of ferrite, the ferrite needles continue to grow and, consequently, the ferrite

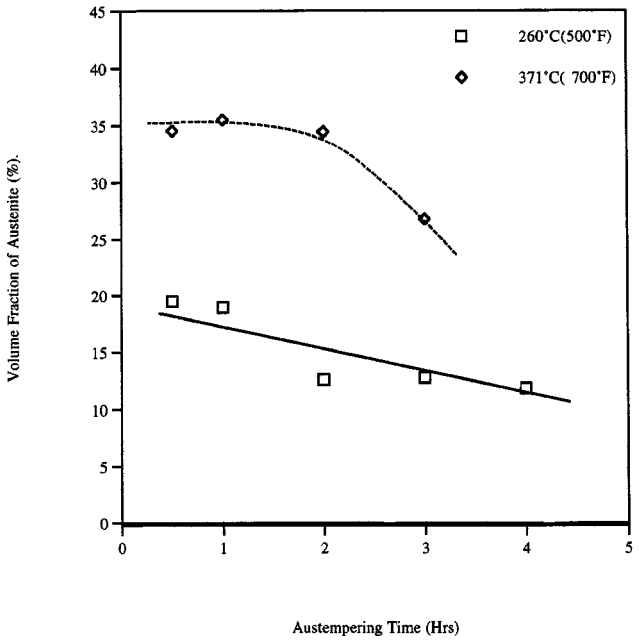


**Fig. 4** Influence of austempering time on the volume fraction of austenite

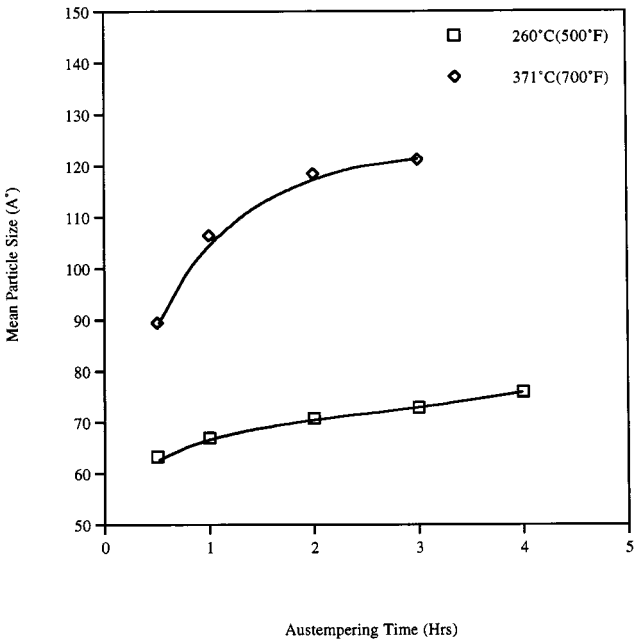


**Fig. 6** Influence of austempering time on the mean particle size ($d$)

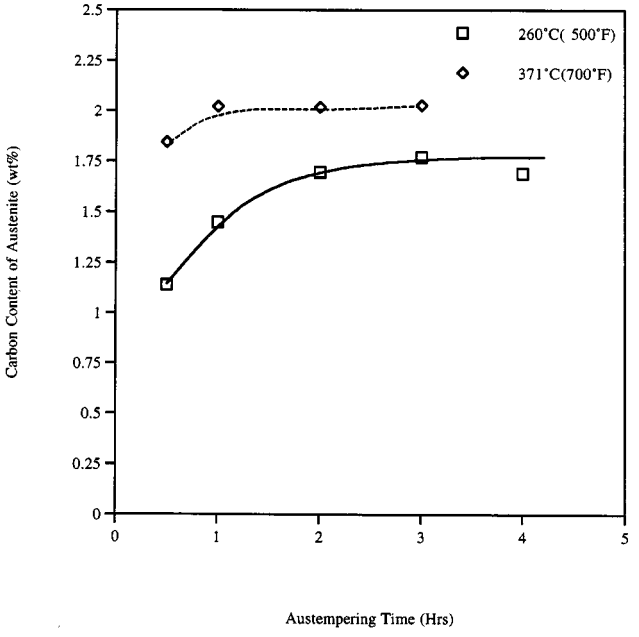


**Fig. 5** Influence of austempering time on the carbon content of austenite (wt.%)

volume fraction increases. Therefore, the austenite volume fraction decreases. On the other hand, at higher temperature (371 °C), austenite content remains more or less constant from 30 min to 2 h of austempering and then starts to decrease. Since carbon content of austenite does not change with time at this temperature (Fig. 5), the austenite volume fraction remains more or less constant at 371 °C with time. The decrease in austenite content at 371 °C after 3 h indicates that probably the stage II reaction has set in or, in other words, the carbide precipitation reaction has just initiated. However, the X-ray plot did not show any carbide peak, which indicates that the amount of carbide is probably too small for detection. Since the "process window" decreases with austempering temperature, 3 h at 371 °C was most probably outside of the process window, while this was not the case at 260 °C.

Figure 5 shows the variation of carbon content of austenite as a function of austempering time in lower and higher bainitic temperature ranges. At the austempering temperature of 260 °C, the carbon content of austenite rises steadily from a low value of 1.1 wt.% at 30 min to 1.7 wt.% after 2 h and continues to increase, although it does so rather slowly. However, at 371 °C, the carbon content was found to be as high as 1.8 wt.% even after a short period of 30 min, increased to about 2% after an hour, and remained practically constant beyond that period. This means two interesting things. First of all, this is an experimental proof that indeed austenite can hold up to 2.0% carbon; and, second, carbon saturation of austenite occurs at 371 °C even at a short duration of time of 1 h, whereas even after 4 h at 260 °C, austenite has not reached the solubility limit of 2% carbon at 260 °C. Carbon enrichment of austenite occurs by diffusion and diffusion is both a time- and temperature-dependent process. However, temperature has a greater influence on diffusion than does time. Therefore, at 260 °C, the temperature being low, diffusion of carbon was very slow, and consequently, carbon content of austenite did not reach the solubility limit of 2% even after 4 h. On the other hand, at 371 °C, a faster diffusion rate of carbon resulted in rapid saturation of austenite with carbon. Present test results also indicate that there is no need to austemper at 371 °C for more than an hour.

For a fixed austempering temperature, the carbon content of austenite ($C_o$) is constant. The carbon content of austenite at a given austenitizing temperature is given by the following equation:[31]

$$C_o = T\gamma / 420 - 0.17(\%Si) - 0.95 \quad \text{(Eq 2)}$$

If we calculate the carbon content of austenite for the present case at 927 °C, it comes out to be $C_o = 0.85$. Out of this, the carbon in the austenite (after austempering) can be taken as $X\gamma C\gamma$, where $X\gamma$ is the volume friction of austenite and $C\gamma$ is the carbon content of austenite. Figure 7 is the plot of $X\gamma C\gamma$ against austempering time at two different temperatures. For the samples austempered at 260 °C, the product $X\gamma C\gamma$ remains practically constant and has a much lower value ($X\gamma C\gamma = 0.26$). This means that the rest of the carbon (0.59%) has remained in ferrite. Part of this will precipitate within the ferritic needles, and the rest of it will produce a super saturated solid solution of bcc ferrite with carbon. The latter carbon will diffuse into austenite given sufficient time and temperature. Therefore, at 260 °C, as the time increases, more carbon diffuses into austenite and, consequently, the carbon content increases. As the carbon content increases, the austenite volume fraction also decreases. Hence, the product $X\gamma C\gamma$ remains more or less constant. This precipitation of carbide will cause significantly higher strength at this temperature, because it will lock up the dislocations in ferrite. It has been recently shown[32] that ADI microstructure contains dislocations and the dislocation density increases with a decrease in the austempering temperature. Therefore, lower austempering temperature has caused not only large dislocation density but also more carbon precipitation within the ferrite. On the other hand, at 371 °C, the product $X\gamma C\gamma$ is of the order of 0.75 after an hour of austempering. This means that after 1 h of austempering, nearly the entire amount of carbon is in the austenite, *i.e.*, very little carbon is precipitated within the ferrite. This has contributed to the lower strength at this temperature. This is also indicative of the fact that a saturation stage has been reached at 371 °C after 1 h of austempering, *i.e.*, nearly the entire carbon is in the austenite at this temperature. Therefore, the carbon content remains more or less constant at this temperature (371 °C) after 1 h. There is a small increase in carbon content from 30 min to 1 h at 371 °C, because the $X\gamma C\gamma$ product at 371 °C after half an hour was low (about 0.66).

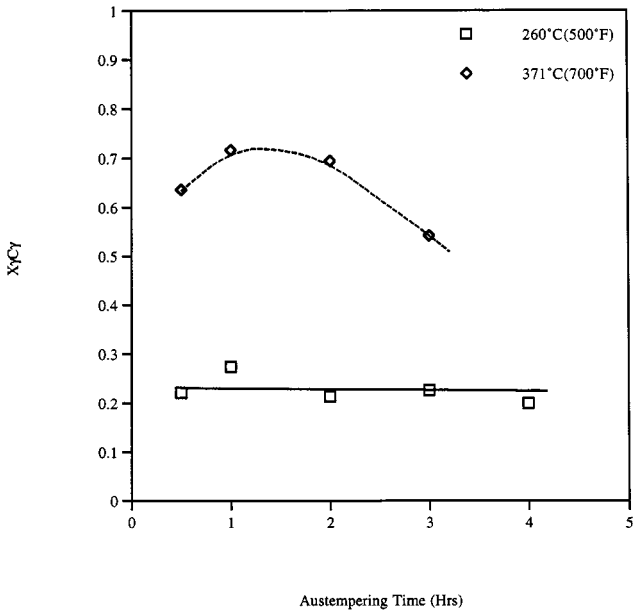


**Fig. 7** Influence of austempering time on the austenitic carbon ($X\gamma C\gamma$)

The volume fractions of austenite formed in the present alloy at 260 and 371 °C after 2 h of austempering are lower than the values reported in the literature on conventional ADI. This is because of the absence of any alloying elements in the ductile iron used in this investigation. Alloying elements, particularly manganese, tend to promote more austenite in the matrix. Since the present alloy did not have any alloying elements and manganese content was also low (0.15%), this has resulted in a lower volume fraction of austenite in the matrix. Rouns and Rundman[33] have studied in detail the microstructure of several ductile irons subjected to different austempering heat treatments. Their results show increasing alloy content increases $X\gamma$ (volume fraction of austenite) and decreases $C\gamma$ (*i.e.*, the carbon content of austenite). For an unalloyed ductile iron austenitized at 871 °C and austempered at 371 °C, they found retained austenite content at 26 vol.% and carbon content 1.98%. Considering our austenitizing temperature is slightly higher than theirs (927 °C vs 871 °C), our values are in close agreement with their test results.

### 3.2 Tensile Properties

The influence of austempering time on yield strength at two different austempering temperatures is reported in Fig. 8, whereas Fig. 9 reports the effect of austempering time on tensile strength of the material at 260 °C and 371 °C, respectively. Lower austempering temperature resulted in much higher strength than that achieved at higher temperature. Like conventional and alloyed ADI, this unalloyed and low manganese ADI also shows that lower ausferrite structure produces higher strength than upper ausferrite structure. While the yield strength increased significantly from a low value of 825 MPa after 30 min of austemper-

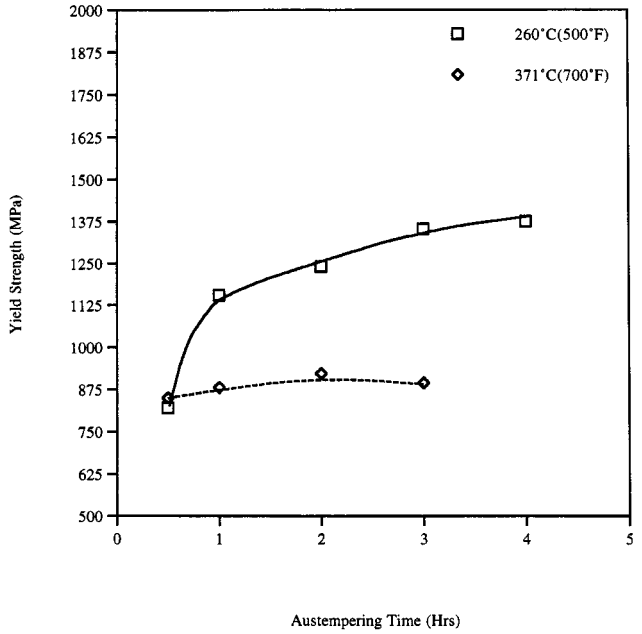


**Fig. 8** Influence of austempering time on the yield strength of low manganese ADI

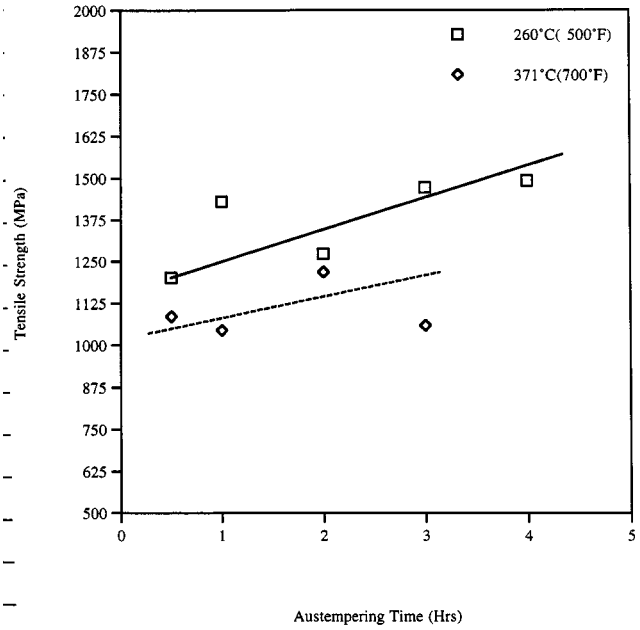


**Fig. 9** Influence of austempering time on the tensile strength (MPa)

ing at 260 °C to a value of 1350 MPa after 4 h, the increase in yield strength was marginal at 371 °C. Table 2 reports the percent elongation of the material as a function of austempering time, at the two austempering temperatures. Though there is some scatter in the data, the trend is obvious. Ductility is higher at higher austempering temperature. This is because the matrix contains more austenite at higher temperature. Because austenite is a tougher phase, when more of it is present, it increases the ductility of the material. However, time has no significant effect on ductility in either upper or lower temperature.

The higher yield and tensile strength at the lower bainitic temperature of 260 °C is directly related to several factors. First of all, at this temperature, both ferrite and austenite are very fine in nature. This fine ferrite and austenite causes higher strength by providing a greater barrier to dislocation motion *via* a Hall-Perch type mechanism.[34,35] Second, as the austempering time increases, the carbon content of the austenite increases. This increases the toughness of the austenite. The higher the carbon content, the tougher will be the austenite because the carbon content will increase its strain hardening rate.[20] Consequently, the strength of the material increases with increasing austempering time at 260 °C. Third, as mentioned earlier, there is a significant amount of carbon precipitation within ferrite at lower termperature, and at this temperature, there also is a large dislocation density in ferrite.[32] Locking up of all these dislocations with carbon will increase the strength of the material. This indeed happens because dynamic strain aging has been reported in ADI. On the other hand, the ferrite and austenite are both very coarse in nature at 371 °C. This causes a reduction in strength of this material at 371 °C. Furthermore, there is very little carbon precipitation within ferrite at this temperature because nearly all of the carbon is in the austenite. Moreover, the dislocation density is also lower. Hence, the strength is lower and no significant increase in strength with time is observed at this temperature. Present test results

**Table 2 Influence of austempering time on the hardness and percentage elongation of low manganese ADI**

| Austempering temperature (°C) | Austempering time (h) | Elongation (%) | Hardness (Rc) |
|---|---|---|---|
| 260 | 0.5 | 1.58 | 46.5 |
| | 1 | 1.60 | 47.8 |
| | 2 | 0.95 | 48.2 |
| | 3 | 1.28 | 48.0 |
| | 4 | 1.25 | 48.9 |
| 371 | 0.5 | 8.20 | 31.5 |
| | 1 | 2.65 | 30.3 |
| | 2 | 5.42 | 33.1 |
| | 3 | 2.84 | 29.7 |

support the authors' earlier observations[18,20–22] in conventional high manganese ADI, that for high strength, ADI must have the following:

- very fine ferrite and austenite,
- a carbon content of austenite as high as possible, and
- a lower value of *d*.

It may not be out of place to point out here the possibility of stress-induced martensite formation in ADI. Because of the high carbon content of austenite, the austenite is highly stable since the higher the carbon content of austenite, the lower is the $M_s$ temperature.[35] For a carbon content of 1.1%, the $M_s$ temperature will be −100 °C. Hence, austentie formed during the austempering process here is expected to be stable at room temperature. There are suggestions in the literature,[36,37] however, that stress-induced martensite forms in ADI and this causes higher strength at lower austempering temperature. Present test results contradict the above suggestions of previous investigators,[36,37] because samples austempered at 260 °C for 30 min had austenite with a carbon content of about 1.1%, whereas samples austempered for 4 h had a carbon content of 1.8%. That means stress-induced martensite is most likely to form in the samples austempered for 30 min. If that is the case, then these samples should have lower fracture toughness since stress-induced martensite will result in a decrease in fracture toughness, making the material more brittle. It is well known that the higher the carbon content of martensite, the more brittle the martensite becomes. Therefore, martensite formed by transformation of such high carbon austenite will definitely make the material brittle and, consequently, will reduce the fracture toughness. As discussed later, the present test results show no significant effect of time on fracture toughness (at 260 °C) even though carbon content of the austenite has increased significantly (Fig. 12). Moreover, microhardness measurement along the fracture surfaces did not show any evidence of martensite being present. Hence, our test results indicate that the higher strength at lower austempering temperature is because of the combination of the following: (a) very fine ferrite and austenite being present at this temperature—the grain size effect; (b) increase in carbon content of austenite, which will increase the strain hardening rate of austenite and its toughness; (c) lower mean free path of dislocation motion; and (d) higher dislocation density together with large carbon precipitation within this ferrite.

### 3.3 Fracture Toughness

Fracture toughness values after austempering for different durations at the two austempering temperatures (260 and 371 °C) are presented in Fig. 10. It is evident that when austempered either at lower or upper bainitic temperatures the fracture toughness remains practically constant, *i.e.*, time has no significant influence on fracture toughness. The fracture toughness values are also comparable to those of hardened and tempered low alloy steels. Test results reported in Fig. 10 show another interesting feature. It is evident that upper ausferritic microstructure provides higher fracture toughness in unalloyed low manganese ADI, whereas the opposite has been found to be true[18–26] in the case of conventional alloyed ADI with higher Mn content. Dorazil and Holzman[38] studied the fracture toughness of unalloyed and low alloyed ADI after austempering at two temperatures, 300 and 400 °C. These results also show higher fracture toughness for upper ausferrite microstructure in unalloyed ADI, while the reverse is found to be true in the case of alloyed ADI. The present test results are therefore in agreement with the observations of Dorazil and Holtzman[38] and other investigations.[18–26]

Retained austenite content is an extremely important factor. Analysis of the test results of the previous investigators[20,21,22] shows that the optimum austenite content for fracture toughness is in the range of 30 to 40%. The results of the present investigation agree well with this. Figure 11 is a plot of austenite content against fracture toughness. The high fracture toughness was obtained in this material when austempering was done at 371 °C in which case the austenite content was between 30 and 36%. Because austenite is a tougher phase, when a fairly large amount of austenite is present, an improvement in the fracture toughness of the material can be expected. Interestingly, if one plots the data of the author's previous study[21] on conventional ADI in the form of austenite content vs fracture toughness, as shown in Fig. 12, that curve also shows that high fracture toughness is obtained when the austenite content is about 30%. While low manganese ADI showed a higher fracture toughness at 371 °C, the conventional ADI had a higher fracture toughness at 302 °C, but both occurred when austenite content

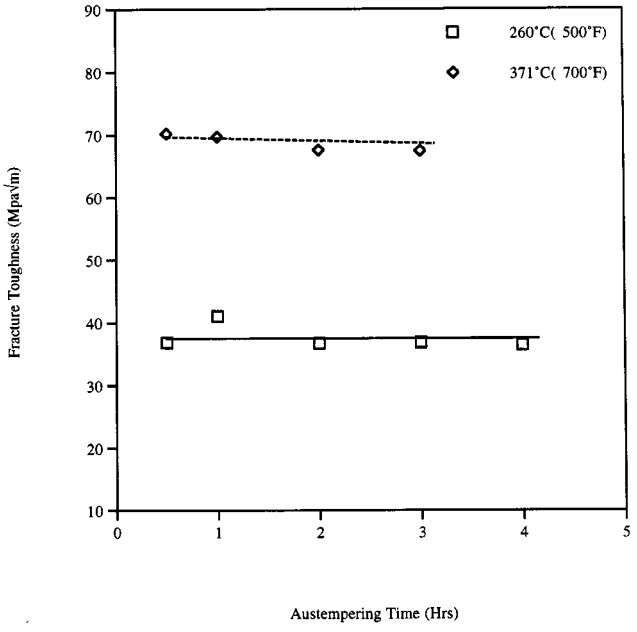


**Fig. 10** Influence of austempering time on the fracture toughness of low manganese ADI

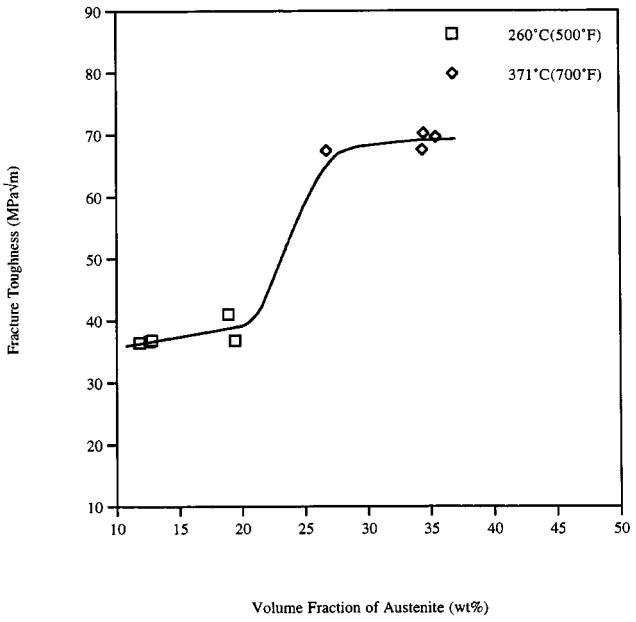


**Fig. 11** Influence of volume fraction of austenite on the fracture toughness of low manganese ADI

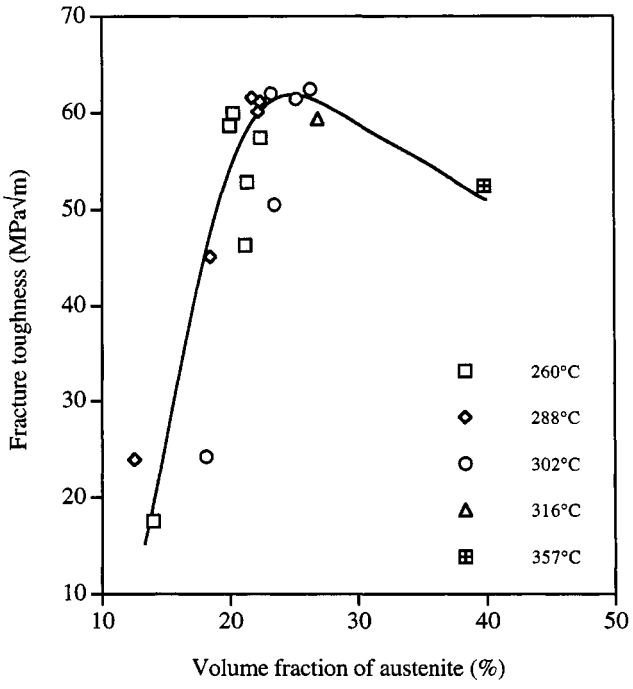


**Fig. 12** Influence of austenite content on fracture toughness of conventional ADI[21]

was about 30 to 36%. Thus, it appears that the optimum austenite content for maximum fracture toughness in ADI should be in this range irrespective of the starting (as-cast) microstructure. The highest fracture toughness in this low manganese ADI was found to be about 70 MPa$\sqrt{m}$, whereas in conventional ADI, the highest fracture toughness was found to be about 60 MPa$\sqrt{m}$ (Fig. 12). This indicates some improvement in fracture toughness in this alloy.

Increasing the toughness of the retained austenite can also lead to increased fracture toughness of the ductile iron as a whole. Increasing carbon content of austenite will increase its toughness as it will result in greater interations[39] between dislocations and carbon atoms. Austenitic carbon ($X\gamma C\gamma$) therefore should be another important factor for fracture toughness of ADI. This parameter ($X\gamma C\gamma$) is a measure of the total carbon content of austenite, which is an indirect measure of the toughness of the austenite phase. Since toughness of austenite will increase with an increase in carbon content, it is expected that fracture toughness should follow a similar relationship. In Fig. 13, the fracture toughness of this material has been plotted in terms of $K_{IC}$ against $X\gamma C\gamma$. It is obvious that the fracture toughness of low manganese ADI increases with an increase in austenitic carbon ($X\gamma C\gamma$), and higher fracture toughness is produced when the product ($X\gamma C\gamma$) is high.

The fracture toughness of ADI should also be dependent on both the (a) austenitic carbon content and (b) mean free path of dislocation motion. Higher austenitic carbon ($X\gamma C\gamma$) will increase its strain hardening rate and, consequently, will increase its fracture toughness. The lower mean free path of dislocation motion will also increase fracture toughness because a smaller grain size is beneficial for fracture toughness.[34,35] Earlier we developed a model[26] that indicates that fracture toughness should be proportional to $(X\gamma C\gamma/d)^{1/2}$. In Fig. 14, the fracture toughness has been plotted against this parameter. Obviously, a increased fracture toughness is obtained as the parameter $(X\gamma C\gamma/d)^{1/2}$ increases at both of the austempering temperatures.

### 3.4 Fractrography

Fractrographs of the samples austempered for different time periods at 260 and 371 °C are shown in Fig. 15 (a) to (d). At lower austempering time, the fracture mode was completely cleavage type, indicative of the brittle fracture as the presence of cleavage facets suggests. On the other hand, at the upper bainitic temperature (371 °C), the fracture mode was mostly ductile since a significant number of dimples appeared on the fracture surface. When fracture surfaces of the samples austempered for different durations were studied, no significant difference in fracture mode was observed. Thus, the fracture mode remained predominantly cleavage type at lower austempering temperature, but at higher temperature, the fracture mode remained mixed (ductile plus cleavage). Since the fracture mode was mostly ductile at higher austempering temperature, this resulted in higher fracture toughness at this temperature (371 °C).

## 4. Conclusions

- The fracture toughness of unalloyed and low manganese ADI with as-cast ferritic structure was higher with upper ausferritic structure than with the lower ausferritic structure.
- A retained austenite content of 30 to 36% is necessary for optimum fracture toughness. Increasing the austempering time at 260 °C increased the yield strength of ADI.
- Lower ausferritic structure produced higher yield and tensile strengths but lower ductility. On the other hand, upper ausferritic structure resulted in lower yield and tensile strength but greater ductility in low manganese ADI.

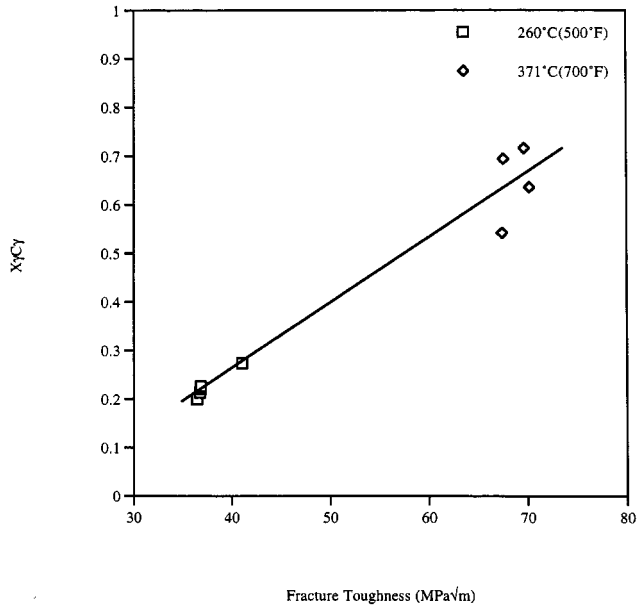


**Fig. 13** Influence of austenitic carbon on the fracture toughness of low manganese ADI

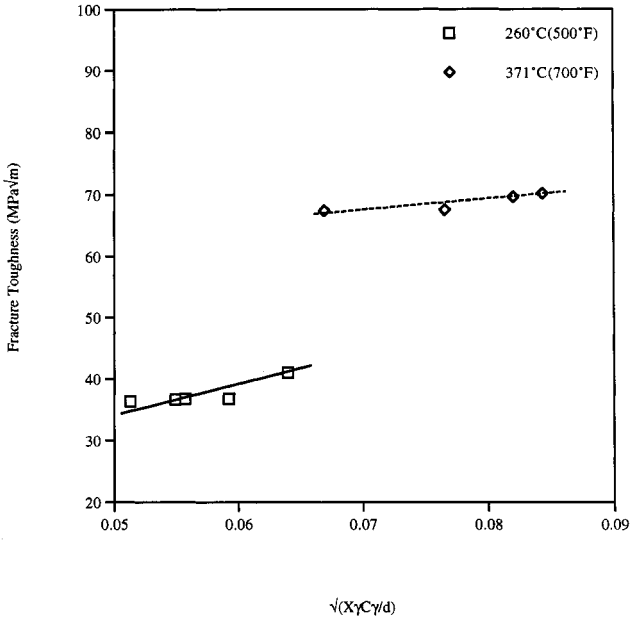


**Fig. 14** Influence of $(X\gamma C\gamma/d)1/2$ on the fracture toughness

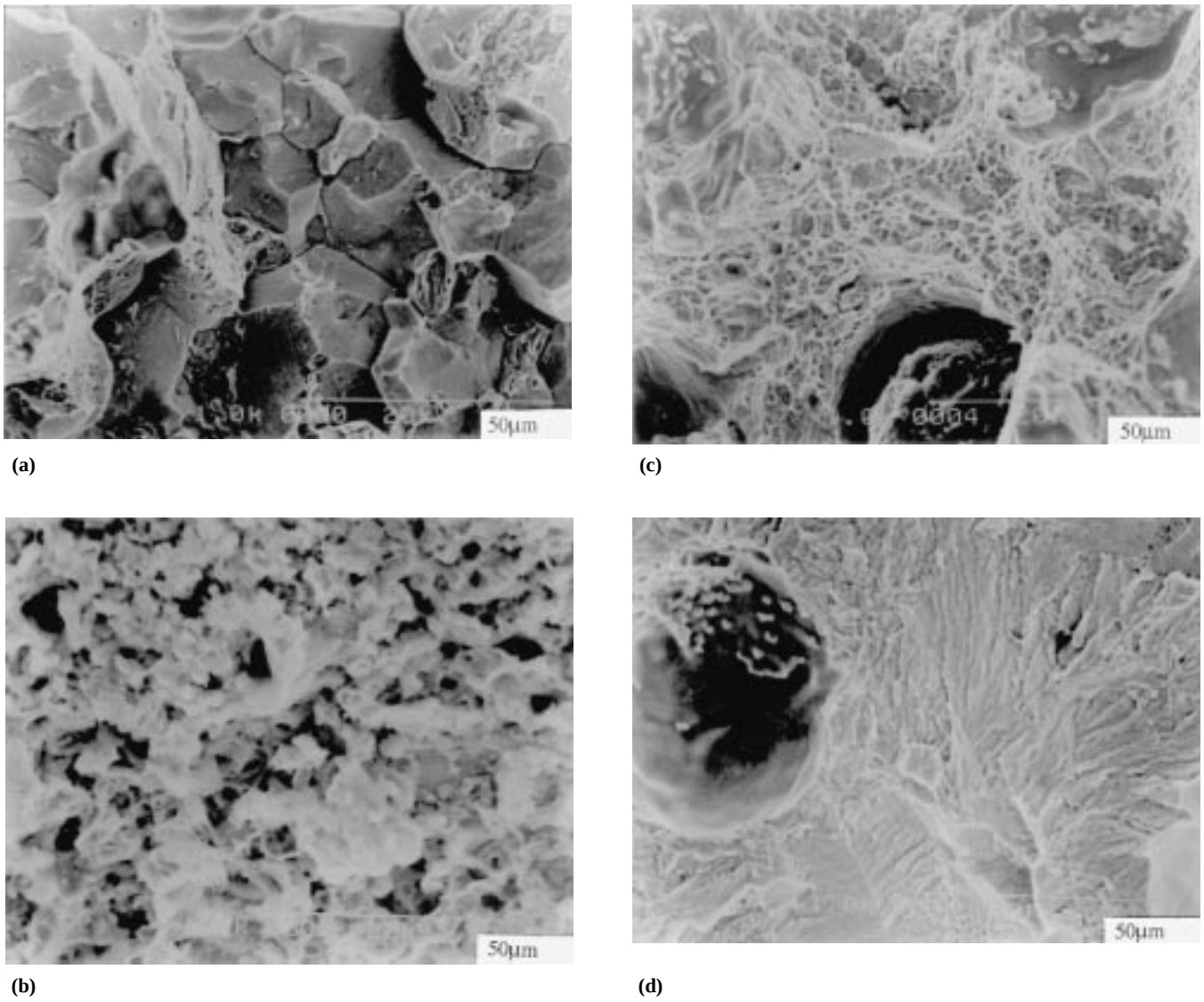


**Fig. 15 (a)** Fractograph of the material austempered at 260 °C for 30 min. **(b)** Fractograph of the material austempered at 260 °C for 2 h. **(c)** Fractograph of the material austempered at 371 °C for 30 min. **(d)** Fractograph of the material austempered at 371 °C for 2 h

- Fracture toughness of this unalloyed low manganese ADI was higher when the austenitic carbon content was high.
- Fracture toughness increases with an increase in the parameter $(X\gamma C\gamma/d)^{1/2.}$

## References


1. J. Dodd: *Modern Casting,* 1978, vol. 68 (5), pp. 60–66.
2. R.B. Gundlach and J.F. Janowak: *Met. Progr.,* 1985, vol. 128 (2), pp. 19–26.
3. R.A. Harding and G.N.J. Gilbert: *Br. Foundaryman* 1986, vol. 79, pp. 489–96.
4. I. Schmidt and A. Schuchert: *Z. Metallk.,* 1987, vol. 78, pp. 871–75.
5. M. Johansson: *AFS Trans.,* 1977, vol. 85, pp. 117–22.
6. L. Bartosiewicz, I. Singh, F.A. Alberts, A.R. Krause, and S.K. Putatunda: *Mater. Characterization,* 1993, vol. 30, pp. 221–34.
7. P. Shanmugam, P.P. Rao, K.R. Udupa, and N. Venkatraman: *J. Mater. Sci.,* 1994, vol. 29, pp. 4933–40.
8. L. Bartosiewicz, A.R. Krause, B. Kovacs, and S.K. Putatunda: *AFS Trans.,* 1994, vol. 92, pp. 117–43.
9. S.K. Putatunda and I. Singh: *Trans. Ind. Inst. Met.,* 1993, vol. 14, pp. 162–83.
10. G. Wilkinson and C. Grupke: *Proc. 2nd Int. Conf. on Austempered Ductile Iron,* Ann Arbor, MI, Mar. 1986, American Foundryman Society, Des Plaines, IL, 1991, pp. 349–58.
11. J. Panasaiewicz, C. Grupke, and J. Huth: *Proc. 2nd World conf. on Austempered Ductile Iron,* Bloomingdale, IL, Mar. 1991, American Foundaryman Society, Des Planes, IL, 1991, pp. 176– 94.
12. K. Okazaski, H. Asai, M. Tokuyoshi, H. Kusoroki, and H. Shakahara: *Proc. 2nd World Conf. on Austempered Ductile Iron,* Bloomingdale, IL, Mar. 1991, American Foundaryman Society, Des Planes, IL, 1991, pp. 288–99.
13. *Annual Book of ASTM Standards,* ASTM Standard E-399, 1996, vol. 03.01, pp. 547–78.
14. J.L. Doong and C.S. Chen: *Fatigue Fract. Eng. Mater. Struct.,* 1989, vol. 12, pp. 155–65.

15. E. Dorazzil and M. Holzman: *Proc. 2nd World Conf. on Austempered Ductile Iron,* Bloomingdale, IL, Mar. 1991, American Foundaryman Society, Des Planes, IL, 1991, pp. 32–66.
16. M. Grench, P. Bowen, and J.M. Young: *Proc. World Conf. on Austempered Ductile Iron,* Bloomingdale, IL, Mar. 1991, American Foundaryman Society, Des Planes, IL, 1991, pp. 338–74.
17. L. Bartosiewicz, I. Singh, F.A. Albert, A.R. Kraurse, and S.K. Putatunda: *J. Mater. Eng. Performance,* 1993, vol. 4, pp. 90–101.
18. S.K. Putatunda and I. Singh: *J. Testing Evaluation,* 1995, vol. 23, pp. 325–32.
19. J. Aranzabal, I. Gutiezzez, J.M. Rodriguezibale, and J.J. Urcola: *Mater. Sci. Technol.,* 1992, vol. 8, pp. 263–73.
20. P.P. Rao and S.K. Putatunda: *Metall. Mater. Trans. A,* 1997, vol. 28A, pp. 1457–70.
21. P.P. Rao and S.K. Putatunda: *Mater. Sci. Technol.,* 1998, vol. 14, pp. 1257–65.
22. P.P. Rao and S.K. Putatunda: *Metall. Mater. Trans. A,* 1998, vol. 29A, pp. 3005–16.
23. J.M. Schissler and J. Saverna: *J. Heat Treating,* 1985, vol. 16, pp. 167–77.
24. J.M. Schissler, J.P. Chobaut, G. Bax, and D. Gonvnel. *Int. Foundry Heat Treatment Conf.,* Johannesburg, South Africa, 1998, pp. 26–30.
25. S.K. Putatunda: *Materials Characterization,* in review.
26. S.K. Putatunda and P. Gadicherla: *Mater. Sci. Eng.,*1999, vol. A268, pp. 15–31.
27. *Annual Book of ASTM Standards,* ASTM Standard E-8, 1998, vol. 0.3.01, pp. 130–45.
28. K.B. Rundman and R.C. Klug: *AFS Trans.,* 1982, vol. 90 pp. 499–503.
29. B.D. Cullity: *Elements of X-ray Diffraction,* Addison-Wesley, Reading, MA, 1974, pp. 411–34.
30. C.S. Roberts: *Trans. AIME,* 1953, vol. 197 pp. 203–06.
31. R.C. Voigt and C.R. Cooper: *Proc. 1st Int. Conf. on Austempered Ductile Iron,* ASM International, Metals Park, OH, 1984, pp. 83–88.
32. V. Franketovic, M.M. Shea, and E.F. Ryntz: *Mater. Sci. Eng.,* 1987, vol. 96, pp. 231–36.
33. T.N. Rouns and K.B. Rundman: *AFS Trans.,* 1988, vol. 96, pp. 851–67.
34. G.E. Dieter: *Mechanical Metallurgy,* 3rd ed., McGraw-Hill, New York, NY, 1986.
35. R.E. Reed: *Hill Physical Metallurgy Principles,* 2nd ed., Van Nostrand Company, New York, NY, 1964.
36. B. Kovacs: *Modern Casting,* 1990, vol. 36, pp. 38–41.
37. P. Mayr *et al.: Proc. 2nd Int. Conf. on Austempered Ductile Cast Iron,* Ann Arbor, MI, Gear Research Institute, Napsville, IL, 1986, pp. 171–78.
38. E. Dorazl and M. Holzmann: *Proc. World Conf. on Austempered Ductile Iron,* Bloomingdale, IL, Mar. 1991, American Foundryman Society, Des Plaines, IL, 1991, pp. 567–75.
39. W.N. Roberts: *Trans. AIME,* 1964, vol. 230, pp. 373–80.